Muon Spin Rotation Studies of Enediynes

Vasily S. Oganesyan,[†,§] Andrew N. Cammidge,[†] Gareth A. Hopkins,[†] Fiona M. Cotterill,[†] Ivan D. Reid,[‡,||] and Upali A. Jayasooriya*[,†]

School of Chemical Sciences and Pharmacy, University of East Anglia, Norwich NR4 7TJ, United Kingdom, Paul Scherrer Institut, CH-5232 Villigen PSI, Switzerland, and Centre for Metalloprotein Spectroscopy and Biology, School of Chemical Sciences and Pharmacy, University of East Anglia, Norwich NR4 7TJ, United Kingdom

Received: August 5, 2003; In Final Form: January 16, 2004

Muon spin rotation spectra of muoniated radicals of the enediyne compounds (*E*)- and (*Z*)-RC≡CCH═CHC≡CR where R = $-CH_2CH_2CH_2CH_3$ are reported and the temperature variation of these spectra from 250 to 400 K investigated. All primary radicals expected were observed and assigned using ab initio DFT calculations. The properties of a six membered secondary radical likely to be formed by the cyclization of the muoniated *Z*-isomer were estimated using an ab initio DFT calculation.

Introduction

Enediyne antitumor antibiotics are a family of compounds discovered from natural product research and rank among the most potent antitumor agents known so far.[1] In the 1980s, it was discovered that a series of naturally occurring antibiotics, including calicheamicin, esperamicin, and dynamicin[2] all possessed this structural motif. The mode of action of these drugs is first via their ability to intercalate into DNA and then due to the enediyne unit which, when activated, cyclizes to produce a highly reactive aromatic diradical. This mode of cyclization was first recognized by Bergman[3] in 1972 and is known as the Bergman cyclization. These diradicals, in turn, are capable of cleaving DNA strands that ultimately leads to cell death.

These biological observations of natural products have encouraged the synthesis of many compounds containing the enediyne "warhead" to be tried as antibiotics.[4] The process of cyclization may be induced both thermally and photochemically to produce the diradical intermediate which is responsible for the hydrogen abstraction reactions from organic substrates.

Muon implantation to produce radical species from unsaturated organic compounds is well established.[5] The acronym μSR stands for muon spin rotation, relaxation, and resonance covering the various ways in which the evolution of the muon polarization is studied. Detection and characterization of radical species with exceptional sensitivity is now possible using spin-polarized muons and single-particle counting techniques.[5] Similar to conventional magnetic resonance, characteristic frequencies provide measurements of internal magnetic or hyperfine parameters. The muon spin plays the role of a nuclear spin, but the spectroscopy proves to be equally sensitive both to muons in electronically diamagnetic environments and to those which experience a hyperfine coupling with paramagnetic electrons, the latter being of importance to the studies involving organic radicals. The chemical reactions of muonium mimic those of atomic hydrogen and form the basis of muonium chemistry. Particularly important in this context are the studies of muonium-substituted organic radicals, formed by muonium addition to double or triple bonds. Also illustrated in the literature are measurements of radical cyclization rates using μSR.[6] The application of μSR to study the cyclizations of enediynes will require the detection and assignment of all possible radicals likely to form with this material. Here we report the first muon implantation study of an enediyne system, where we have detected all of the possible primary radicals that are formed and they are identified and assigned with the help of ab initio DFT calculations. The hyperfine parameters of a secondary radical likely to result from the radical cyclization of the *Z*-isomer are also calculated and reported. A strategy for the study of the prodrugs themselves, where the R groups are much more complicated, is suggested via the monitoring of the secondary radicals.

Experimental Section

Synthesis. Initial attempts to synthesize hex-3-en-1,5-diyne, the simplest member of the enediyne family of compounds, in large enough quantities for muon work, proved to be dangerous. *n*-Butyl groups were therefore used to replace the terminal hydrogens on the alkyne groups. The enediyne synthesis utilized the Stephens-Castro coupling of terminal alkynes in the presence of a palladium(0) catalyst and copper(I) iodide. This is a two step reaction involving sequential addition of the alkyne to each end of dichloroethene, in the case of both cis (*Z*) and trans (*E*) isomers. The method used is that of Chemin and Linstrumelle.[7] The purity of the final compounds was confirmed by high-field ^{1}H NMR spectroscopy.

Spectroscopy. TF-μSR measurements were made using the GPD spectrometer on the μE4 decay muon beamline at the Paul Scherrer Institute, Villigen, Switzerland. The liquid samples were sealed into 35 mm o.d. thin-walled Pyrex ampules, following deoxygenation by five freeze−pump−thaw cycles. The samples were mounted in a cryostat and exposed to the beam of spin-polarized positive muons while an external magnetic field of 0.2 T was applied transverse to the muon (spin)

* To whom correspondence should be addressed. Fax: +44 (0)1603 592003. E-mail: u.jayasooriya@uea.ac.uk.

† School of Chemical Sciences and Pharmacy, University of East Anglia.

‡ Paul Scherrer Institut.

§ Centre for Metalloprotein Spectroscopy and Biology, School of Chemical Sciences and Pharmacy, University of East Anglia.

|| Present address: Electrical & Computer Engineering, Brunel University, Uxbridge, Middlesex UB8 3PH, United Kingdom.

10.1021/jp0362990 CCC: $27.50
Published on Web 02/17/2004

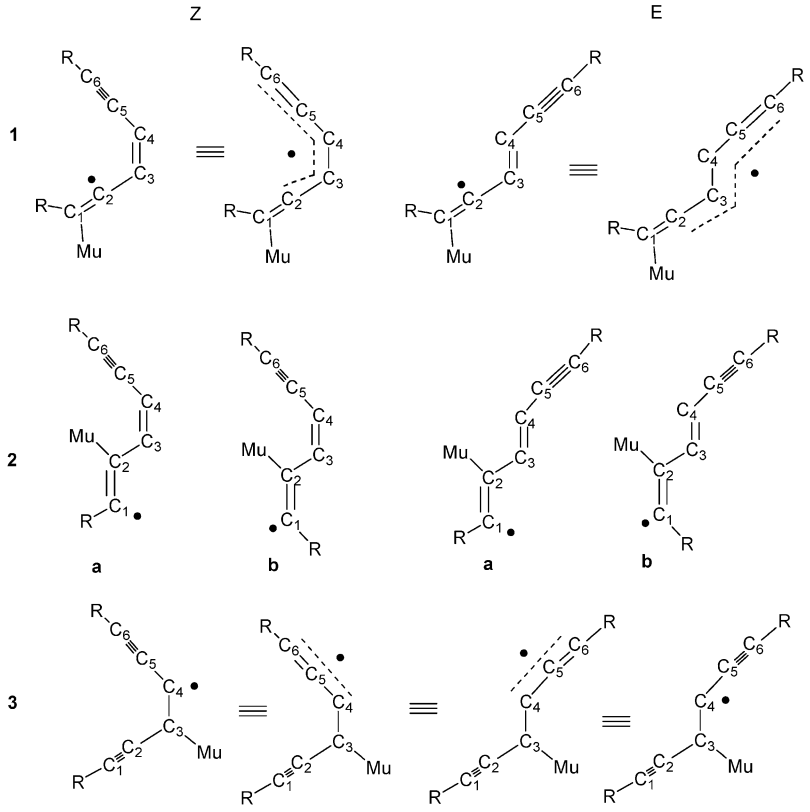

Figure 1. (a) All of the distinct primary radicals expected from muonium addition to the *Z* and *E* isomers. Rows 1 and 2 are those arising from addition to a triple bond and the row 3 from addition to the double bond. The hydrogen atoms connected to C_3 and C_4 are omitted for clarity.

beam direction. To correlate a positron decay with a muon incident on the sample, the experiment was run in time differential mode in which the incoming muon starts a clock at $t = 0$ and in so doing triggers a gate signal of 10 μs length (a few muon lifetimes) during which no further muons can be counted. When the decay positron of the muon is measured at time *t*, then a count at time *t* is added to the histogram for the given detector in which the positron was detected. While limiting the count rate of events to ca. 5×10^4 muons per second, this technique provides the necessary time resolution to measure relatively high muon spin rotation frequencies of radicals (up to ca. 500 MHz).

Typically, 9×10^7 to 10×10^7 good decay events were accumulated in 4 data histograms for the *Z* compound, whereas only about 5×10^7 to 6×10^7 good decay events were accumulated for the *E* compound. The data were analyzed by fitting the usual theoretical function in Fourier space, which allowed the determination of the muon precession frequencies.[8] The diamagnetic component was filtered out in the analysis in order to avoid overlap with the radical signals.

Ab initio DFT Computational Details. The calculations described in this work were performed on a Linux/Pentium III based workstation using the Amsterdam Density Functional (ADF) program, version 2000.0.1.[9] The local exchange-correlation approximation (LDA) of Vosko, Wilk, and Nusair[10] was used. The final results show that this level of approximation gives predictions of the desired physical quantities with sufficient accuracy for these molecules. Inclusion of the non local gradient corrections of Becke[11] for exchange and Perdew[12] for correlation changes the calculated values of hyperfine couplings only slightly (<10%). All molecular calculations were of spin-unrestricted type, so as to allow for substantial spin-polarization on atoms. An uncontracted triple-ζ basis set (ADF basis set IV) with a single set of polarization functions was used for all atoms. In particular, carbon atoms were modeled with triple-ζ 2s, 2p, and one 3d polarization function and hydrogen and muonium atoms were with triple-ζ 1s and one 2p polarization function. All geometry optimizations were performed, at the same level of theory, using the algorithm of Versluis and Zeigler.[13] Starting geometries were calculated using molecular mechanics (MM) force field methods.[14]

Results and Discussion

The six unsaturated carbon atoms of the enediyne chain consist of three symmetry equivalent pairs, thus giving only three unique addition sites each for muonium in the (*E*)- and (*Z*)-tetradec-7-en-5,9-diyne molecules. The radicals that result from the addition of muonium across the triple bonds are numbered 1 and 2, with radical 3 for addition to either end of the double bond. All possible radicals are shown in Figure 1 for the *Z* and *E* isomers. Clearly the adducts across the double bond (3Z) are identical, predicting only one radical frequency for both *Z* and *E* isomers. 1Z and 1E adducts are predicted to have only one conformer, and hence only one frequency, because the unpaired electron is expected to be delocalized along the π bonding backbone of the molecules, as shown in Figure 1. Rotation of this radical about the C_1C_2 bond results in two stable isomers with almost identical hyperfine coupling, as shown in Figure 6a. The structure pairs 2Z(a), 2Z(b) and 2E-(a), 2E(b) are related by a rotation about the C_1C_2 bond, which is a formal double bond that separates the unpaired electron from the muon. These radicals a and b have the radical electron trans and cis with reference to the muon, and thus are expected to show significantly different hyperfine constants. However, only one hyperfine frequency is experimentally found for this radical center, vide infra. Therefore, the minimum energy optimized conformer as shown in Figure 2 is used for the

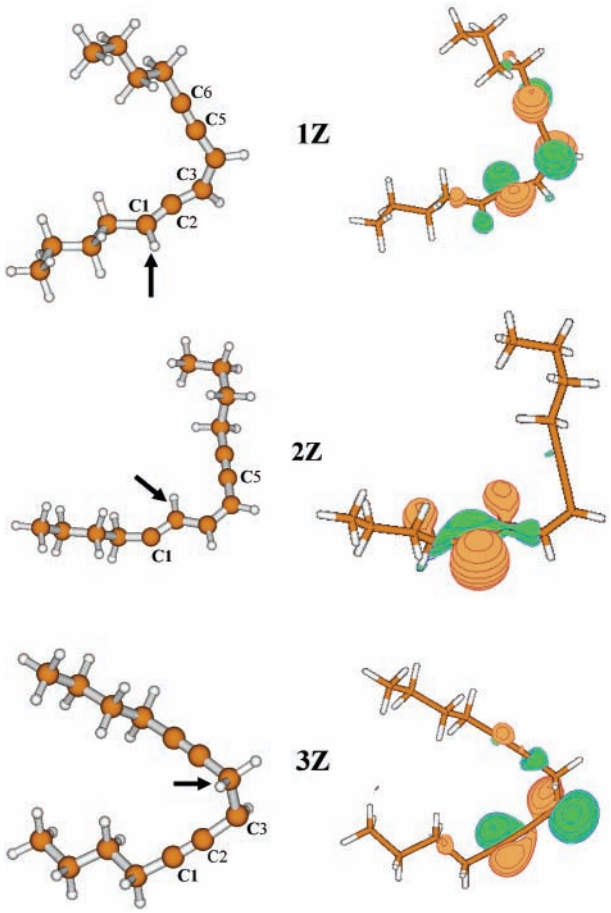

Figure 2. Geometry optimized for minimum energy radicals from the *Z* isomer together with their SOMOs. Mu positions are indicated by arrows.

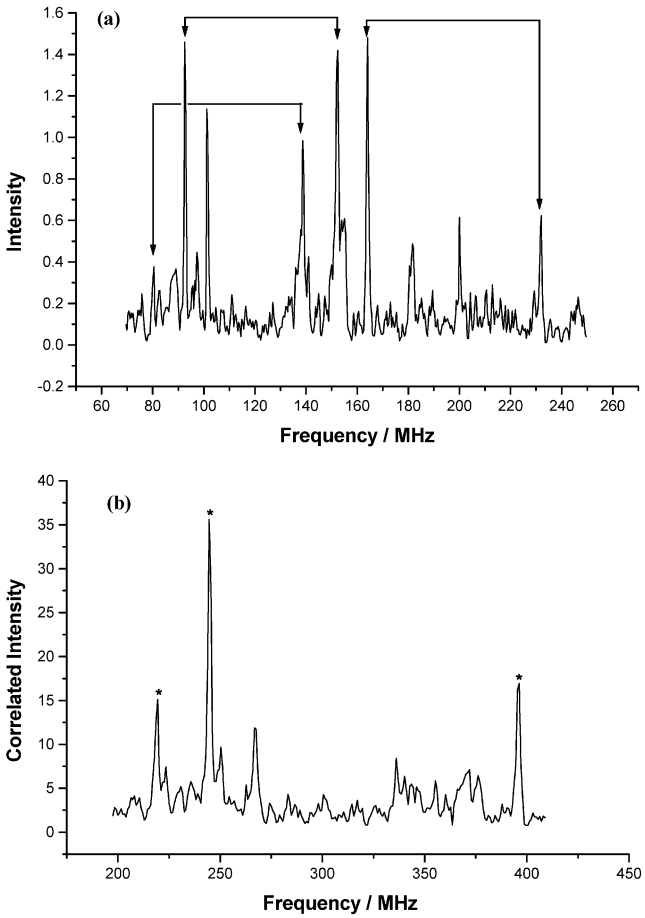

Figure 3. (a) TF-μSR spectrum recorded during the implantation of positive muons into (*Z*)-tetradec-7-en-5,9-diyne, neat liquid at 330 K and with a magnetic field of 0.2 T. (b) Correlation plot confirming the three radical species. [Note that the signal at 100 MHz in (a) is a cyclotron clock signal, and the other features that do not correlate are spurious peaks.]

calculations for this radical that are to follow. All of the optimized geometries, which are in very good agreement with the conformations presented in Figure 1, and the unpaired electron spin distributions of the three resulting radicals are shown in Figure 2.

Figure 3a shows the TF-μSR spectrum recorded during the implantation of positive muons into (*Z*)-tetradec-7-en-5,9-diyne neat liquid at 330 K. Six precession frequencies from three radical species are observed, as shown by the pairs of arrows. To a first approximation, the radical pairs appear at $(n_\mu \pm 1/2A_\mu)$ where n_μ is the bare muon precession frequency (27 MHz at 0.2 T) and A_μ is the radical hyperfine interaction, so the identification of one precession frequency determines where its matching signal can be found. This allows spurious peaks in the spectrum to be disregarded along with other known artifacts such as harmonics of the proton cyclotron (most noticeable at 101 MHz). Using a precise formula for the position of the radical frequencies,[15] one can calculate correlations between potentially matching frequencies and plot the result to help discriminate between small signals and noise.[16] The radical assignments are confirmed by the correlation plot given in Figure 3b (where one must ignore the apparent correlation near 260 MHz caused by the strong 101 MHz harmonic). If one were to consider the probable extent of delocalization of the unpaired electron in each of the radicals shown in Figure 2, significant differences in the hyperfine interactions are to be expected and are indeed observed. The observed radical frequencies are 219.0, 244.8, and 396.0 MHz.

TF-μSR spectrum of the *E* isomer, neat liquid at 295 K, is shown in Figure 4a, with the correlation plot in Figure 4b. Similar to the *Z* isomer, three adducts are expected and are observed with hyperfine frequencies of 225.4, 235.2, and 398.5 MHz.

The calculations were performed using an ab initio technique based on density functional theory, with the local spin density approximation. Inclusion of the generalized gradient approximation in the DFT calculations led only to minor alterations of the calculated hyperfine coupling constants for muonium.

Vacuum-state muonium has the value of hyperfine coupling $A \sim 4.5$GHz, which is greater than that for the hydrogen atom by the approximate ratio of the magnetic moment of the muon to proton of 3.18:1. However, in host materials, the muonium hyperfine parameter is sensitive to the local chemical environment and is determined by the delocalization of the unpaired electron and the amount of unpaired electron density on muonium (muonium 1s orbital's contribution to the molecular orbital of the unpaired electron). Consequently, one would expect much lower values of hyperfine coupling parameters for muonium associated with a host molecule. The hyperfine coupling tensor is normally described by the magnitudes of the three principal components and their orientation with respect to the molecular frame of coordinates, by three Eulerian angles. The anisotropy of the tensor arises through dipole−dipole interaction of the muon spin with the unpaired electron spin density, while the isotropic part is due to the so-called "contact term" which depends on the electron spin density at the nucleus (or in this case by the hyperconjugation effect). The calculations

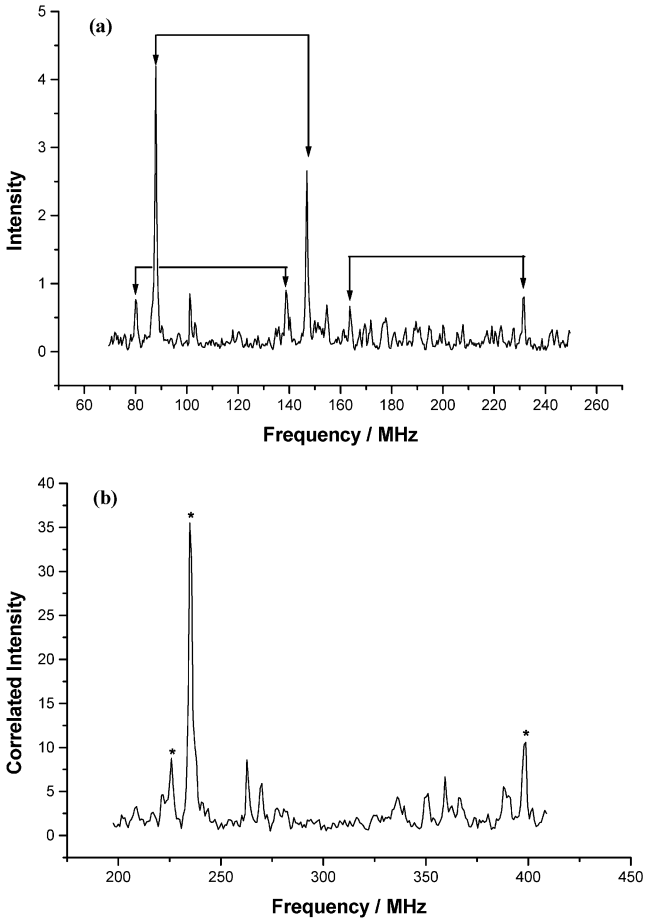

Figure 4. (a) TF-μSR spectrum recorded during the implantation of positive muons into (*E*)-tetradec-7-en-5,9-diyne, neat liquid at 330 K and with a magnetic field of 0.2 T. (b) Correlation plot confirming the three radical species. [Note that the signal at 100 MHz in (a) is a cyclotron clock signal, and the other features that do not correlate are spurious peaks.]

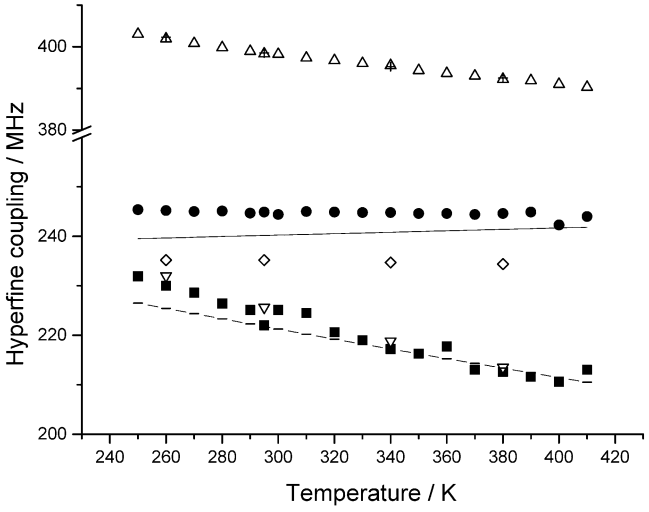

Figure 5. Temperature variation of the hyperfine interactions of all of the muoniated radical species. Experimental observations are given by ● for 1Z; △ for 2Z; ■ for 3Z; + for 1E; ◇ for 2E, and ▽ for 3E. Theoretical prediction for 1Z is shown as a line and the broken line for theoretical prediction for the 3Z isomer radical.

revealed that the hyperfine coupling of all six muoniated enediyne radicals are predominantly isotropic with only slight anisotropy, arising from a dipole−dipole interaction of the muon spin with the unpaired electron delocalized on neighboring atoms (mostly 2p-orbitals of C atoms). The calculated values of the hyperfine coupling tensor components of the three muoniated *Z* radicals are given in Table 1. The corresponding values for *E* radicals are almost identical to those calculated for *Z* radicals. The orientation of the hyperfine tensors in all these radicals are such that A_{11} is perpendicular to the $C_{(radical)}-C-Mu$ plane, whereas A_{22} and A_{33} are on this plane.

The spectra of these compounds were run as neat liquids, and therefore, it is the rotationally averaged isotropic hyperfine interactions that are measured by these experiments. The values estimated by the DFT calculation were used in the assignment given in Table 1. The calculated values of the hyperfine coupling constants of the radicals 1Z to 3Z are in reasonably good agreement with the experimental values.

Spectra were also collected at about ten-degree intervals from 250 to 400 K for the *Z* isomer, and only four measurements were made for the *E* isomer at 260, 295, 340, and 380 K, due to beamtime limitations.

Although the radicals 1Z and 3Z have similar values of hyperfine coupling, their temperature variation of the hyperfine frequencies are markedly different, Figure 5. This is what one would intuitively expect, since the radical 3Z(3E) involves the opening of the double bond with the muonium addition. The resulting single bond can thus almost freely rotate (Figure 6b), whereas the radical 1Z(1E) has the muonium addition to the triple bond resulting only in a double bond that is still highly restricted to rotation about the bond axis (Figure 6a). In contrast, the hyperfine coupling constant of the 2Z(2E) radical is almost twice that of the other two, and its hyperfine frequency is almost temperature independent.

The temperature dependence of the hyperfine interactions of these radicals may be due to two dynamic processes. An inversion about the radical center and rotations about the bond separating the muon and the unpaired electron. In the case of vinyl free radicals, there is evidence of a low energy inversion process about the radical center via a tunneling mechanism.[17] The enediynes investigated in the present study have very bulky substituents (*n*-butyl groups) that make such a tunneling process of inversion unlikely, but an inversion of the whole molecule about the radical center is still likely. However, an inspection of the radical center of the optimized structure of 3Z shows that it is almost flat with the dihedral angle between the C4−H bond and the C3C4C5 plane being 178°, thus eliminating an inversion about the radical center as the cause of the observed temperature variation of the hyperfine coupling. This leaves the second possibility of a rotation about the bond between the muon and the unpaired electron as the probable candidate for this temperature dependence.

To distinguish between the two types of radicals 1Z(1E) and 3Z(3E) and to confirm the arguments presented in the earlier paragraphs, theoretical studies were performed on the effect of rotation around the C_1C_2 double bond (the most significant perturbation of the hyperfine interaction) of the 1Z radical (Figure 6a) and the C_3C_4 single bond (the most significant perturbation of the hyperfine interaction) of the 3Z radical (Figure 6b), on the total bonding energy and the hyperfine coupling of these radicals. Since the *Z* and *E* isomers show a similar pattern of hyperfine coupling behavior, DFT calculations on internal rotations were performed only on the *Z* system. Bond lengths and angles were taken from the globally optimized geometries. Total bonding energy and the hyperfine coupling constants as a function of the above rotations for the isomers 1Z and 3Z are shown in Figure 6. Calculations were for every 10° rotation angle. Radical 1Z is found to possess an energy

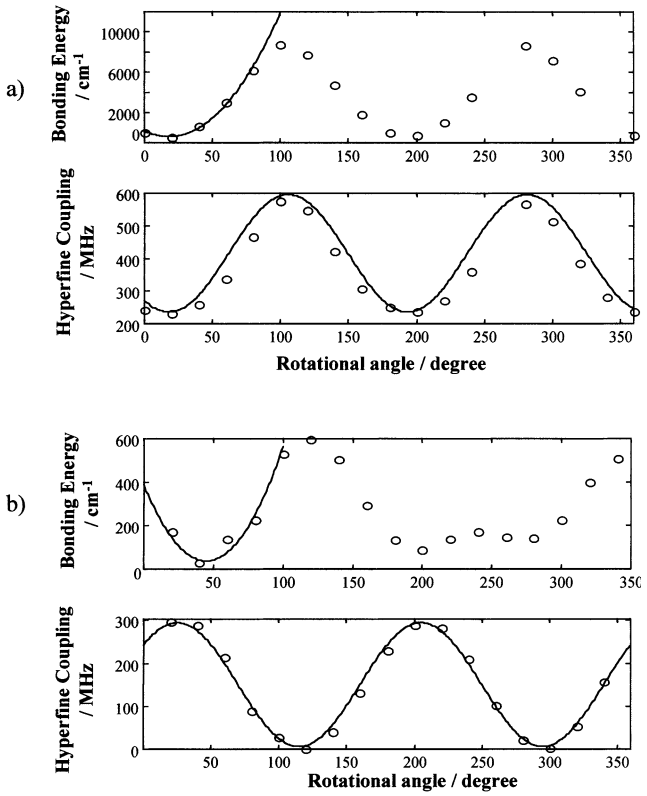

Figure 6. Total bond energy and hyperfine coupling as a function of rotational angle for rotation about the bonds that formally separate the unpaired electron from the Mu atom for the isomers (a) 1Z for rotation about the C_1C_2 bond and (b) 3Z for rotation about the C_3C_4 bond.

TABLE 1: DFT Calculated Values of the Hyperfine Coupling Tensor Components of the Isomer, (*Z*)-Tetradec-7-en-5,9-diyne

	hyperfine Interactions/MHz				
isomer	A_{11}	A_{22}	A_{33}	$\bar{A}_{(\text{theor})}$[a]	$\bar{A}_{(\text{exp})}$
1Z	234	237	255	244 (241)	245
2Z	462	474	498	474	396
3Z	222	225	252	234 (220)	219

[a] The values represent the mean average of the three principal components of *A* tensor. The values in brackets are the corrected ones after the effect of rotation about the C3−C4 bond at 330 K has been included in the theoretical calculation. The experimental data are those collected at 330 K. The values for the E isomer are identical to those of the Z isomer within 2−3 MHz.

surface with two minima and two barriers to rotation of equal height. In contrast, the 3Z isomer has its second minimum split into two, with three barriers to rotation of different heights in energy to each other. Note that for the 3Z isomer, the *Z*−*E* interconversion is via these torsional barriers.

A semiclassical approach, assuming a simple harmonic potential for rotation about this bond, was used to predict the variation in hyperfine coupling constant with temperature. This is a reasonable approximation for rotation about the double bond where the activation energy is high. In the report by Ramos et al.[20] on the studies of muoniated ethyl radicals, a cosine potential has been used for the case of rotation about a single bond. However, as we will show below, the harmonic oscillator model is sufficient in the present case to produce results which are in excellent agreement with experiment. In the case of the 1Z isomer, the torsional oscillations around 15° are well approximated by the kinetic equation for an idealized harmonic potential, Figure 6

$$\ddot{\Theta} = -\omega^2\Theta \qquad \omega = \sqrt{2k/I}$$

with the simple solution

$$\Theta(t) = \sqrt{E/k}\,\sin(\omega t) \qquad E = \frac{I\dot{\Theta}^2}{2} + k(\Theta - \Theta_0)^2$$

where E is the total energy, k is a force constant, and I is the moment of inertia. Variation of the hyperfine coupling can be approximated by a cosinusoidal dependence:

$$A(t,E) \sim A_0 + A\cos\left(2(\sqrt{E/k}\sin(\omega t) - \Theta_A)\frac{\pi}{180}\right)$$

Numerical averaging over a period of oscillation τ gives the dependence of hyperfine interaction on the total energy

$$\langle A(E)\rangle = \frac{1}{\tau}\int_0^\tau A(t,E)\,\mathrm{d}t$$

Both numerical integrations result in simple exponential dependencies of the form

$$\langle A(E)\rangle_{iZ} = a_{iZ}\exp(b_{iZ}E)$$

where $a_{1Z} = 236$ MHz, $b_{1Z} = 8.47 \times 10^{-5}$ cm and $a_{3Z} = 257$ MHz, $b_{3Z} = -7.75 \times 10^{-4}$ cm, for 1Z and 3Z, respectively. A positive value of b_{1Z} indicates an increase of the hyperfine coupling with increase in energy for 1Z, whereas the relatively larger negative value of b_{3Z} indicates a significant decrease of the hyperfine coupling for 3Z.

Further, averaging of $A(E)$ using Boltzmann statistics and the fact that $b_{iz}kT < 1$ results in the following general expression for the temperature dependence of hyperfine coupling of radicals 1Z and 3Z, respectively

$$\langle A(T)\rangle_{iZ} = \frac{a_{iz}}{1 - b_{iz}kT}$$

In the case of the 1Z radical both the bonding energy and hyperfine coupling show almost periodic dependence with the same period and in phase, Figure 6a. Therefore one would expect a similar temperature variation for the first and second minima of the total energy surface. However in the case of the 3Z radical the second minimum of the bond energy has a more complex structure, Figure 6b. Nevertheless, the hyperfine coupling repeats the same behavior in the vicinity of the second minimum, rotation angle around 200°, as it has near the first minimum. Therefore, qualitatively the same temperature variation is to be expected for both minima. Predicted temperature variations of hyperfine frequencies for radicals 1Z and 3Z are compared with the experimental measurements and found to show excellent agreement, Figure 5.

In the case of the 1Z radical, the bonding energy resisting rotation is substantial as anticipated for a π bond that exists between the C1 and C2. This also results in significant delocalization of the unpaired electron on to the neighboring carbon atoms as shown in Table 2 and Figures 1 and 2. The most significant gross orbital populations of the unpaired electron for carbon atoms are 23.2%, 37.2%, and 23.0% for C2, C4, and C6, respectively, leaving only ∼4% for the 1s orbital of muonium. The large torsional barrier (force constant $k = 1.840$ cm^{-1} deg^{-2}) for this bond separating the muon from the unpaired electron also makes it impossible to detect any

TABLE 2: Calculated Principal Values of Hyperfine Coupling Tensors and the Most Significant Gross Populations of Unpaired Electron Density of 1s Orbital of Muonium and 2p Orbitals of Carbon Atoms at Two Different Rotation Angles around the Double/Single Bond[a]

	A_{11}	A_{22}	A_{33}	A_{av}	C1(2p)	C2(2p)	C3(2p)	C4(2p)	C6(2p)	μ(1s)
1Z 20^0	222	225	243	231		23.2%		37.2%	23%	3.82%
1Z 100^0	558	570	603	576		67%		4.5%		10.7%
2Z 0^0	462	474	498	475	62.1%	2.1%				10.25%
2Z 100^0	444	453	482	456	61.6%					11.37%
3Z 40^0	276	282	306	286	34.4%		48.2%			4.23%
3Z 120^0	−11	−8	18.3	∼0	33.1%		48.2%			∼0%

[a] Contributions of less than 2% are not shown.

significant change with temperature of the hyperfine coupling constant for the temperature interval between 240 and 400 K as demonstrated in Figure 5.

The situation for the 3Z isomer is somewhat different. The delocalized π-orbital density of carbon atoms is concentrated in only one-half of the molecule and the double bond is fully opened to give a single bond with muonium addition, making for almost free rotation around it and hence a very low total energy barrier to rotation. However, rotation around this bond will result in different orientations of the muonium 1s orbital relative to the 2p orbital of the neighboring carbon (C4 if muon is at C3) containing the unpaired electron. As a consequence of this variation in overlap of these orbitals, the unpaired electron density on muonium is different for different angles of rotation (see Table 2). The latter effect thus changes the hyperfine coupling constant from ∼300 MHz at the energy minimum to nearly zero MHz at around a rotation angle of 110°, Figure 6b. This, combined with the low energy barrier ($k \sim 0.173$ cm^{-1} deg^{-2}) to rotation, is expected to result in a noticeable decrease of hyperfine coupling constant with increase in temperature, as observed experimentally (Figure 5).

Unpaired electron density in the 2Z radical is almost completely localized in one-half of the molecule, mainly on an sp^2 type orbital of C1. Only one radical frequency is experimentally observed (Figures 3 and 4), and the optimized structure of this radical is the trans isomer, as shown in Figure 2. This reduced π delocalization is responsible for the larger unpaired electron density on the muonium 1s orbital of this radical, ca. 10.25% of the unpaired electron. This explains the increased value of the hyperfine coupling constant, of 420 MHz of the 2Z radical at 330 K, compared to 241 and 230 MHz (ca. 4% of the unpaired electron) respectively for the 1Z and 3Z radicals.

Assuming that it is more likely to result in a six membered ring compared to a four or five membered ring by cyclization, 2Z is the appropriate candidate for such a reaction. However, the possibility exists of other types of secondary radical formation. A complete investigation of such secondary reactions will involve further calculations and RF-MuSR experiments, which are planned for the future. The present investigation is concluded by calculating the structure and unpaired electron distribution of this predicted six-membered secondary radical. The hyperfine tensor components for this radical are $A_{11} = 6.3$ MHz, $A_{22} = 11.4$ MHz, $A_{33} = 15.9$ MHz, and $A_{av} = 11.2$ MHz. The globally optimized structure together with its unpaired electron density distribution are shown in Figure 7. Comparison of this structure with that of the parent 2Z structure, both calculations for isolated molecules in the gas phase, shows an energy advantage of ca. 60 kcal mol^{-1} for cyclization.

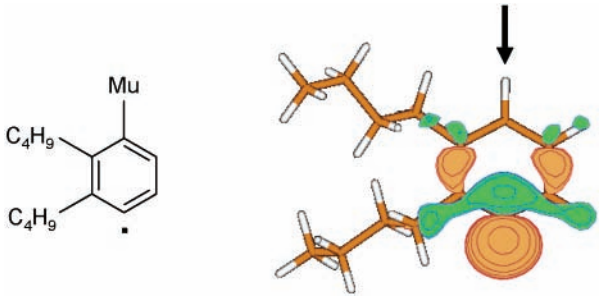

Figure 7. Optimized structure and the unpaired electron distribution, obtained by the DFT calculation, of the secondary radical likely to be formed by the cyclization of the primary muoniated radical 2Z. Muonium position is indicated by an arrow.

Conclusions

This investigation was initiated with the intention of measuring the hyperfine properties of all of the radicals that are likely to be formed by the implantation of muons into this very basic model of the active template of an enediyne prodrug. For each group of isomers there are three sites of muon addition to a molecule which can result in different values of hyperfine coupling. A detailed density functional theory calculation was performed which includes prediction of temperature variations of the hyperfine interactions expected for different radicals. All radicals predicted for both isomers were observed and assigned. DFT calculations on globally optimized structures confirm that appropriate Z and E isomers have similar hyperfine couplings. Temperature variations of the hyperfine couplings predicted from DFT calculations using the harmonic oscillator model for rotations about C−C bonds are in excellent agreement with experimental data and confirms the assignments proposed in this study.

There are several reports of vinyl radicals in the literature with the first measurement by Cochran et al.[17] where the radical was created by photolysis of a solid argon matrix containing acetylene and hydrogen chloride. μSR of such radicals has been reported by Rhodes et al.[18,19] where A_μ values of 591.4 and 732.4 MHz were found for bis(trimethylsilyl)acetylene and 389.3 and 334.1 MHz for diphenyldiacetylene. The latter values are in agreement with those measured for the 2Z and 2E radicals in the present study. The values for the 1Z and 1E radicals in the present report have significantly lower hyperfine couplings because of the higher degree of delocalization of the unpaired electron across the molecule.

It is interesting to note that the calculations predict almost identical values of hyperfine parameters for the pairs of isomeric radicals 1Z and 1E, 2Z and 2E and 3Z and 3E. These predictions are in good agreement with experiment except in the case of 1Z and 1E isomers (Figure 5) where the values are significantly different by a few percent right across the experimental temperature range. The DFT calculations are for the optimized structural geometry which shows all isomers to have slightly nonplanar carbon skeletal backbones. The observed differences in the hyperfine parameters between 1Z and 1E isomers that is not modeled by the above calculations may be a consequence of the neglect of molecular dynamic processes, particularly the

rotation about the C2−C3 formally single bond. These dynamic processes are clearly important at the high temperatures of these experiments, and it is reasonable to expect slight differences in the extent of resulting perturbations of the delocalization of the unpaired electron across the molecule for these two conformers. This therefore may be the explanation of the slightly lower hyperfine parameters observed for the 1(E) isomer compared to those of the 1(Z) isomer.

There was no lifetime broadening of radical signals observed suggesting the secondary reactions to be outside the μSR time window for this particular system under the conditions used in the experiment, as was anticipated. Comparison of the samples, before and after the experiment, show definite colorations indicating either cyclization or polymerization.

The compounds of this family that have significant drug potency have much more elaborate R groups with substantially more unsaturated sites for muonium addition. These adducts are also likely to have hyperfine frequencies in the same region as those reported here for the enediyne moiety. However, the hyperfine parameters estimated for the secondary "cyclic" radical are rather small and are well separated from any interfering primary radical frequencies. Therefore, monitoring the secondary radical would be a viable strategy for studying cyclizations in the more complex molecular systems. This should be possible with the newly developed RF-μSR facilities. The RF-μSR technique should also provide access to more dilute solutions, thus making it possible to discriminate between cyclization and polymerization. The cylisation rates which could be measured using muon implantation, by necessity, are those for a mono-radical. However the Bergman cyclization produces diradicals, but it will be of interest to investigate for the presence of a correlation between these two types of cyclization in order to facilitate the use of μSR spectroscopies for the study of Bergman type of cylisation. Such studies are currently in progress.

Acknowledgment. We thank the Paul Scherrer Institute, Villigen, Switzerland for the muon facilities and the EPSRC, U.K. for funding the research, BBSRC for supporting V.S.O., and together with the Rutherford Appleton Laboratory for a CASE studentship to G.A.H. Professor Sandy McKillop is thanked for the inspiration for this project. We thank a referee for useful comments.

References and Notes

(1) See, for example; (a) Review: Maier, M. E. *Synlett* **1995**, 13. (b) *Enediyne Antibiotics as Antitumor Agents*; Borders, D. B., Doyle, T. W., Eds.; Marcel Dekker: New York, 1995. (c) Arya, D. P.; Warner, P.; Jebaratnam, D. A. *Tetrahedron Lett*. **1993**, *34*, 7823. (d) Arya, D. P.; Devlin, T. A.; Jebaratnam, D.; Warner, P. U.S. Patent No. 5,770,736, June 1998. (e) Xi, Z.; Goldberg, I. H. In *Comprehensive Natural Products Chemistry*; Barton, D. H. R., Nakanishi, K., Eds.; Pergamon: Oxford, U.K., 1999; Vol. 7, p 553.

(2) (a) Nicolaou, K. C.; Zuccarello, G.; Ogawa, Y.; Schweiger, E. J.; Kumazawa, T. *J. Am. Chem. Soc.* **1988**, *110*, 4866. (b) Nicolaou, K. C.; Ogawa, Y.; Zuccarello, G.; Kataoka, H. *J. Am. Chem. Soc.* **1988**, *110*, 7247. (c) Magnus, P.; Carter, P. A. *J. Am. Chem. Soc.* **1988**, *110*, 1626. (d) Russell, K. C.; Kim, C. *J. Org. Chem.* **1998**, *63*, 8229. (e) Konig, B.; Pitsch, W. *J. Org. Chem.* **1996**, *61*, 4258. (f) Nicolaou, K. C.; Maligress, P.; Shin, J.; De Leone, E.; Rideout, D. *J. Am. Chem. Soc.* **1990**, *112*, 7825. (g) Semmelhack, M. F.; Neu, T.; Foubelo, F. *Tetrahedron Lett.* **1992**, *33*, 3277.

(3) Bergman, R. G.; Jones, R. R. *J. Am. Chem. Soc.* **1972**, *94*, 660.

(4) See, for example: (a) Konishi, M. *Antibiot* **1989**, *42*, 1449. (b) Maier, M. E. *Synlett* **1995**, *1*, 13. (c) Smith, A. L.; Nicolaou, K. C. *J. Med. Chem*. **1996**, *39*, 2103. (d) Black, K. A.; Wilsey, S.; Houk, K. N. *J. Am. Chem. Soc*. **1998**, *120*, 5622. (e) Kaneko, T.; Takahashi, M.; Hirama, M. *Tetrahedron Lett*. **1999**, *40*, 2015. (f) *Comprehensive Organic Synthesis*; Trost, B. M., Fleming, I., Semmelhack, M. F., Eds.; Pergamon Press: New York, 1991; Vol 4.

(5) Walker, D. C. *Muon and Muonium Chemistry*; Cambridge University Press: New York, 1983. Roduner, E. *Lecture Notes in Chemistry*; Springer: Heidelberg, 1988; Vol. 49. Muon Science. Muons in Physics, Chemistry and Materials. *Proceedings of the 51st Scottish Universities Summer School in Physics*; Lee, S. L., Kilcoyne, S. H., Cywinski, R., Eds.; 1988. For journal special issues on this topic, see: *Appl. Magn. Reson.* **1997**, 13; *Magn. Reson. Chem.* **2000**, 38.

(6) (a) Burkhard, P.; Roduner, E.; Hochmann, J.; Fischer, H. *J. Phys. Chem.* **1984**, *88*, 773. (b) Burkhard, P.; Roduner, E.; Fischer, H. *Int. J. Chem. Kinet.* **1985**, *17*, 83. (c) Strub, W.; Roduner, E.; Fisher, H. *J. Phys. Chem.* **1987**, *91*, 4379.

(7) Chemin, D.; Linstrumelle, G. *Tetrahedron* **1994**, *50*, 5335.

(8) (a) Roduner, E. *Chem. Soc. Rev*. **1993**, 337. (b) Roduner, E.; Fischer, H. *Chem. Phys*. **1981**, *54*, 261. (c) Roduner, E.; Brinkman, G. A.; Lourier, W. F. *Chem. Phys.* **1982**, *73*, 117.

(9) (a) Baerends, E. J.; Ellis, D. E.; Ros, P. *Chem. Phys.* **1973**, *2*, 41. (b) Versluis, L.; Ziegler, T. *J. Chem. Phys.* **1988**, *88*, 322. (c) Velde, G. te.; Baerends, E. J. *J. Comput. Phys*. **1992**, *99*, 84. (d) Fonseca Guerra, C.; Snijders, J. G.; Velde, G. te.; Baerends, E. J. *Theor. Chem. Acc.* **1998**, *99*, 391.

(10) Vosko, S. H.; Wilk, L.; Nusair, M. *Can. J. Phys.* **1980**, *58*, 1200.

(11) Becke, A. D. *J. Chem. Phys.* **1986**, *84*, 4524.

(12) Perdew, J. P.; Chevary, J. A.; Vosko, S. H.; Jackson, K. A.; Pederson, M. R.; Singh, D. J.; Fiolhais, C. *Phys. Rev. A* **1992**, *46*, 6671.

(13) Versluis, L.; Ziegler, T. *J. Chem. Phys.* **1988**, *322*, 88.

(14) Woo, T. K.; Cavallo, L.; Ziegler, T. *Theor. Chem. Acc.* **1998**, *100*, 307.

(15) Roduner, E.; Fischer, H. *Chem. Phys.* **1981**, *54*, 261.

(16) Reid, I. D.; Roduner, E. *Struct. Chem.* **1991**, *2*, 419.

(17) Cochran, E. L.; Adrian, F. J.; Bowers, V. A. *J. Chem. Phys.* **1964**, *40*, 213.

(18) Rhodes, C. J.; Symons, M. C. R.; Scott, C. A.; Roduner, E.; Hemings, M. *J. Chem. Soc., Chem. Commun.* **1987**, 447.

(19) Rhodes, C. J.; Morris, H.; Reid, I. D. *Hyperfine Interact.* **1997**, *106*, 203.

(20) Ramos, M. J.; McKenna, D.; Webster, B. C.; Roduner, E. *Faraday Trans. 1* **1984**, *80*, 267.